ChemComm



COMMUNICATION

View Article Online



A porous supramolecular ionic solid†

Cite this: Chem. Commun., 2021. **57**, 7248

Received 27th May 2021, Accepted 24th June 2021

DOI: 10.1039/d1cc02806e

rsc.li/chemcomm

Nathan Jackson, b Irma Rocio Vazquez, b Ying-Pin Chen, Yu-Sheng Chen and Wen-Yang Gao **

We report a synthetic strategy to integrate discrete coordination cages into extended porous materials by decorating opposite charges on the singular cage, which offers multidirectional electrostatic forces among cages and leads to a porous supramolecular ionic solid. The resulting material is non-centrosymmetric and affords a piezoelectric coefficient of 8.19 pC N⁻¹, higher than that of the wurtzite ZnO.

Discrete coordination cages, also known as metal-organic cages or metal-organic polyhedra, constructed by the selfassembly of metal ion or clusters and organic ligands, 1-3 have recently garnered significant attention as a class of permanently porous materials.4-6 Structural designability and modularity, similar to that of MOFs, 7,8 along with solution processibility, enable families of coordination cages to be investigated in gas storage/separation, 2 catalysis, 10,11 and drug delivery. 12 Given their large internal cavities and tunable diversified structures, coordinate cages have been viewed as supramolecular building blocks to build infinite porous framework materials. 13-15 In order to achieve the extended frameworks, two well-known strategies¹⁶ have been investigated: (1) pillaring linkers to bridge unsaturated metal sites of coordination cages (Fig. 1a);^{17–19} (2) mechanical bonds, including interlocking and interpenetrating, to expand the dimension (Fig. 1b).²⁰⁻²² Recently, Bloch et al. reported an example of porous ionic solids based on the self-assembly of two different types of coordination cages carrying opposite charges (Fig. 1c).²³

Herein, we report a new synthetic strategy of decorating charges on the building blocks (e.g., organic ligands), which results in charge separation on the singular coordination cage and enables to extend coordination cages into a permanently porous material. An ionic solid is composed of cations and anions held together by electrostatic forces. Our strategy introduces opposite charges to separated sites of the singular supramolecular coordination cage, which offers multidirectional electrostatic forces among cages and leads to an ordered close-packing supramolecular ionic solid (Fig. 1d).

We initiated these investigations by choosing an organic ligand featuring a motif (e.g., pyridine-3,5-dicarboxylic acid) resembling isophthalic acid, commonly encountered in the assembly of coordination cages. 24,25 Meanwhile, to exemplify the proof-of-concept, we employed the N-methylation of pyridine via iodomethane to introduce the positive charge to the ligand. Therefore, we synthesized 3,5-dicarboxy-1-methylpyridinium chloride (1) as the ligand (Fig. 2a), starting from pyridine-3,5-dicarboxylic acid followed by esterification, N-methylation, and hydrolysis (see details in ESI†). The solvothermal reaction of 1 and Cu(OAc)2·H2O in the presence of N,N-dimethylformamide (DMF) and methanol at 75 °C for 24 hours provides blue block-shaped crystals of 2 (Fig. 2b). In contrast, the same reaction condition with pyridine-3, 5-dicarboxylic acid, instead of 1, does not afford any crystalline phase (Fig. S1, ESI†).

Single-crystal X-ray diffraction (SCXRD) analysis reveals that 2 crystallizes in the cubic space group of $I\overline{4}3m$ (a = 20.746(3) Å, Table S1, ESI†) with an empirical formula of [Cu₁₂(OCH₃)₁₂ $(C_8H_6O_4N)_{12}(H_2O)_4$]. As shown in Fig. 3a and b, the metal cluster is composed of two square-pyramidal Cu(II) cations bridged by two μ₂-methoxide anions. While an aqua ligand partially occupies the axial position of the square pyramid pointing toward the inside, each Cu(II) also coordinates with two oxygen atoms of two carboxylate groups from different ligands in a cis mode, which generates a basal plane with two oxygen atoms of the methoxide ions. Overall, each metal cluster

^a Department of Chemistry, New Mexico Institute of Mining and Technology, Socorro, New Mexico 87801, USA. E-mail: wenyang.gao@nmt.edu

^b Department of Mechanical Engineering, University of New Mexico, Albuquerque, New Mexico, 87106, USA

^c NSF's ChemMatCARS, The University of Chicago, Lemont, Illinois, 60439, USA † Electronic supplementary information (ESI) available: Experimental details, spectra, X-ray crystallographic information, and additional figures and tables. CCDC 2085461. For ESI and crystallographic data in CIF or other electronic format see DOI: 10.1039/d1cc028066

Communication

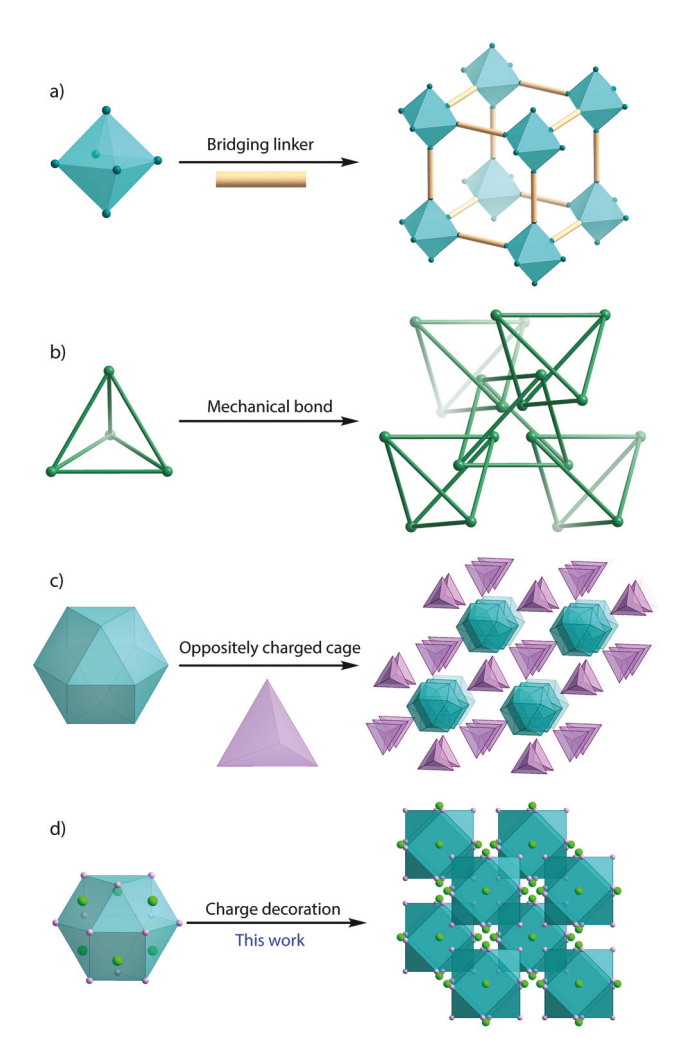


Fig. 1 (a) Pillaring linkers are added to bridge unsaturated metal sites of discrete coordination cages (unsaturated metal sites). (b) Mechanical bonds, such as interlocking and interpenetrating, are built to extend the frameworks. (c) Electrostatic forces between oppositely charged coordination cages construct a porous material. (d) Here we report that electrostatic forces between different sites of the singular cage (, sites carrying opposite charges) build a porous supramolecular ionic solid.

Fig. 2 (a) The synthetic steps of 3,5-dicarboxy-1-methylpyridinium chloride (1). Conditions: (i) EtOH, H2SO4, 78 °C, 24 h. (ii) MeI, toluene, MeCN, 65 °C, 24 h. (iii) HCl, 90 °C, 72 h. (b) Solvothermal reaction of ${\bf 1}$ and Cu(OAc)₂·H₂O affords blue blocked-shaped crystals of 2.

with a formula of $[Cu_2(OMe)_2(OOC)_4(H_2O)_{0.7}]^{2-}$ (Fig. 3b) carries two negative charges. Each positively charged pyridinium moiety connects two metal clusters via the carboxylate groups.

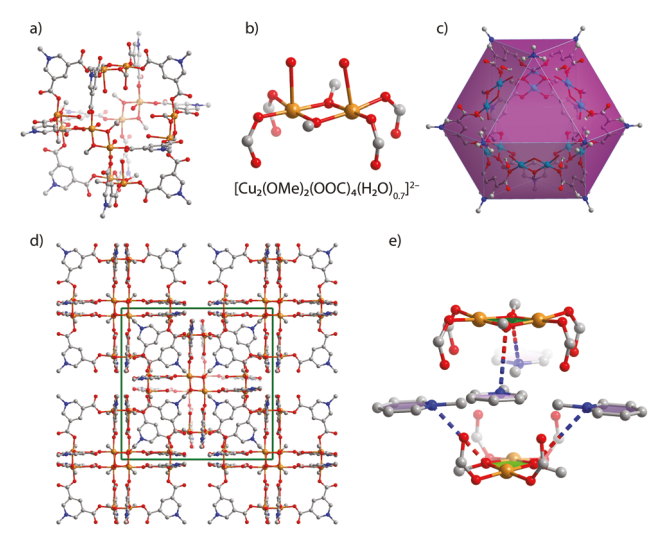


Fig. 3 (a) The discrete coordination cage, 2, is built from the solvothermal reaction of ${\bf 1}$ and Cu(OAc)₂·H₂O. (b) The metal cluster, [Cu₂(OMe)₂(OOC)₄ $(H_2O)_{0,7}]^{2-}$, carries negative charges. (c) A cuboctahedron is formed by connecting the twelve positively charged nitrogen sites and the six negatively charged metal clusters are distributed at the centres of the six square faces of the cuboctahedron. (d) The discrete cages follow a body-centred cubic packing mode. (e) The electrostatic forces between different sites in the ionic solid are illustrated by dotted lines, drawn by the positive sites and their closest negative sites (the axial agua ligands were omitted for clarity).

Thus, the discrete coordination cage is constructed by six negatively charged metal clusters (including twelve methoxide anions and aqua ligands, respectively) and twelve positively charged organic ligands (Fig. 3a). A cuboctahedron can be generated by connecting the twelve positively charged nitrogen sites, while the six negatively charged metal clusters are distributed at the centres of the six square faces (Fig. 3c). Separated charge distribution at the vertices or on the faces of the polyhedron directs the packing of the coordination cages in the 3-dimensional space. The multidirectional electrostatic forces between cages result in a supramolecular ionic solid with a body-centred cubic packing (Fig. 3d). The electrostatic forces between different sites in the ionic solid are illustrated in Fig. 3e.

Powder X-ray diffraction (PXRD) analysis verifies the phase purity of 2, based on the agreement between the experimental patterns and the calculated ones (Fig. S2, ESI†). Meanwhile, the obtained supramolecular ionic solid, 2, exhibits distinctive chemical stability after being soaked for one week in a series of different organic solvents, e.g., acetonitrile (MeCN), acetone, dichloromethane (CH2Cl2), methanol (MeOH), and tetrahydrofuran (THF), probed by PXRD patterns (Fig. 4a). In addition, the desolvated sample obtained by extensive acetonitrile exchange and evacuation at 90 °C still demonstrates consistent PXRD patterns (Fig. S2, ESI†), compared with the initial ones.

Based on these observations, 2 was activated by exhaustive acetonitrile exchange followed by heating at 90 °C under vacuum prior to gas adsorption analysis. The permanent porosity of 2 was characterized by N2 adsorption isotherms at 77 K (Fig. 4b), which provided a measured Brunauer-Emmett-Teller

ChemComm Communication

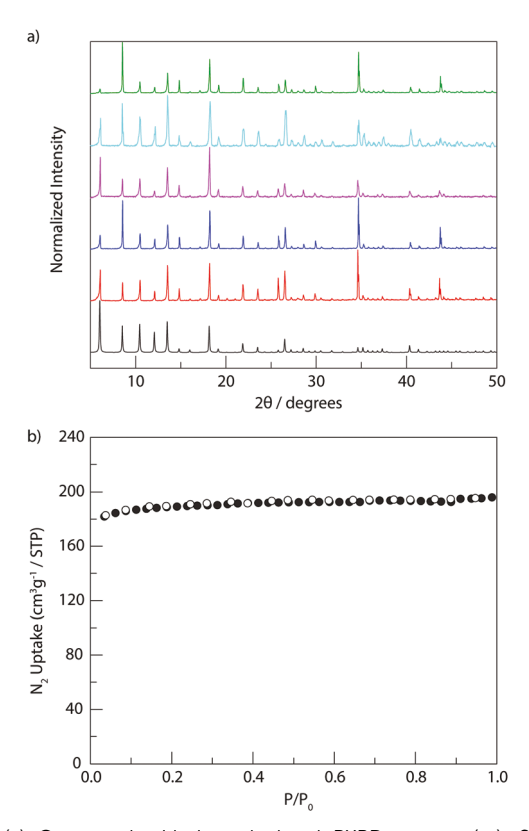


Fig. 4 (a) Compared with its calculated PXRD pattern (-), 2 shows consistent PXRD patterns after being soaked for one week in a series of organic solvents, including MeCN (—), acetone (—), CH₂Cl₂ (—), MeOH (—), and THF (—). (b) N₂ adsorption isotherms of **2** (adsorption (●), desorption (O)) were measured at 77 K. Its Brunauer-Emmett-Teller (BET) surface area was generated with a value of 690 m² g⁻¹ $(P/P_0 = 0.02 - 0.15).$

(BET) surface area of 690 m² g⁻¹ ($P/P_0 = 0.02-0.15$). Though the multidirectional electrostatic forces lead to a close-packing solid of 2, it still exhibits permanent porosity due to the empty internal space of coordination cages and their ordered packing (Fig. S3, ESI†).

Piezoelectric materials, which convert mechanical stress into electrical energy (and vice versa), are crucial in energy storage, sensors, actuators, and others. 26,27 Given the noncentrosymmetric space group and the remarkable chemical stability of 2, we examined its piezoelectric response using a Berlincourt piezometer (details in ESI†). Multiple measurements provide an average piezoelectric coefficient, d_{33} value, of 8.19 (± 1.30) pC N⁻¹. To validate the measurement, the same analysis method provides a d_{33} value of 4.30 pC N⁻¹ for the wurtzite zinc oxide (ZnO) powder, consistent with the reported value on ZnO in the range of 3-12 pC N⁻¹. ²⁸ To the best of our knowledge, 2 represents the first coordination cage reported with a piezoelectric response, which may expand the scope of well-explored traditional piezoelectric materials.

In conclusion, we report a new synthetic strategy of charge decoration to extend discrete coordination cages into a supramolecular ionic solid. While multidirectional electrostatic forces between positively charged ligands and negatively charged metal nodes among cages lead to a close packing, the empty internal space of the coordination cage still provides the permanent porosity of the resultant solid. Meanwhile, we describe its piezoelectric response, which outperforms that of the ZnO powder. The emerging metal-organic materials may provide promising potentials as a new class of piezoelectric materials, in addition to the well-known pure inorganic materials.

W. Y. G. acknowledges the start-up fund of New Mexico Tech. N. J. acknowledges partial support from U.S. Department of Defense (DoD) Army Research Office (No. 76064-RT-RFP). Single-crystal data of 2 were acquired at NSF's ChemMatCARS. NSF's ChemMatCARS Sector 15 is supported by the Divisions of Chemistry (CHE) and Materials Research (DMR), National Science Foundation, under grant number NSF/CHE-1834750. Use of the Advanced Photon Source, an Office of Science User Facility operated for the U.S. Department of Energy (DOE) Office of Science by Argonne National Laboratory, was supported by the U.S. DOE under Contract No. DE-AC02-06CH11357. We thank Junyu Ren (University of North Texas) for the thermogravimetric analysis.

Conflicts of interest

There are no conflicts to declare.

References

- 1 T. R. Cook and P. J. Stang, Chem. Rev., 2015, 115, 7001.
- 2 M. M. Smulders, I. A. Riddell, C. Browne and J. R. Nitschke, Chem. Soc. Rev., 2013, 42, 1728.
- 3 M. Han, D. M. Engelhard and G. H. Clever, Chem. Soc. Rev., 2014, 43, 1848.
- 4 M. M. Deegan, A. M. Antonio, G. A. Taggart and E. D. Bloch, Coord. Chem. Rev., 2021, 430, 213679.
- 5 A. J. Gosselin, C. A. Rowland and E. D. Bloch, Chem. Rev., 2020, 120, 8987.
- 6 S. Mollick, S. Fajal, S. Mukherjee and S. K. Ghosh, Chem. Asian J., 2019, 14, 3096.
- 7 H. Furukawa, K. E. Cordova, M. O'Keeffe and O. M. Yaghi, Science, 2013, 341, 1230444.
- 8 H. C. Zhou and S. Kitagawa, Chem. Soc. Rev., 2014, 43, 5415.
- 9 J. R. Li and H. C. Zhou, Nat. Chem., 2010, 2, 893.
- 10 C. M. Hong, R. G. Bergman, K. N. Raymond and F. D. Toste, Acc. Chem. Res., 2018, 51, 2447.
- 11 W.-X. Gao, H.-N. Zhang and G.-X. Jin, Coord. Chem. Rev., 2019,
- 12 D. Zhao, S. Tan, D. Yuan, W. Lu, Y. H. Rezenom, H. Jiang, L.-Q. Wang and H.-C. Zhou, Adv. Mater., 2011, 23, 90.
- 13 J. J. Perry IV, J. A. Perman and M. J. Zaworotko, Chem. Soc. Rev., 2009, 38, 1400.
- 14 F. Nouar, J. F. Eubank, T. Bousquet, L. Wojtas, M. J. Zaworotko and M. Eddaoudi, J. Am. Chem. Soc., 2008, 130, 1833.
- 15 A. J. Cairns, J. A. Perman, L. Wojtas, V. C. Kravtsov, M. H. Alkordi, M. Eddaoudi and M. J. Zaworotko, J. Am. Chem. Soc., 2008, 130, 1560,
- 16 L. Chen, Q. Chen, M. Wu, F. Jiang and M. Hong, Acc. Chem. Res., 2015, 48, 201.
- 17 H. N. Wang, X. Meng, G. S. Yang, X. L. Wang, K. Z. Shao, Z. M. Su and C. G. Wang, Chem. Commun., 2011, 47, 7128.
- 18 E. J. Gosselin, G. R. Lorzing, B. A. Trump, C. M. Brown and E. D. Bloch, Chem. Commun., 2018, 54, 6392.
- 19 J.-R. Li, D. J. Timmons and H.-C. Zhou, J. Am. Chem. Soc., 2009,
- 20 L. Jiang, P. Ju, X. R. Meng, X. J. Kuang and T. B. Lu, Sci. Rep., 2012, 2, 668.

Communication ChemComm

- 21 X. Kuang, X. Wu, R. Yu, J. P. Donahue, J. Huang and C.-Z. Lu, Nat. Chem., 2010, 2, 461.
- 22 J. Heine, J. S. auf der Günne and S. Dehnen, J. Am. Chem. Soc., 2011, **133**, 10018.
- 23 E. J. Gosselin, G. E. Decker, A. M. Antonio, G. R. Lorzing, G. P. A. Yap and E. D. Bloch, J. Am. Chem. Soc., 2020, 142, 9594.
- 24 B. Moulton, J. Lu, A. Mondal and M. J. Zaworotko, Chem. Commun.,
- 25 M. Eddaoudi, J. Kim, J. B. Wachter, H. K. Chae, M. O'Keeffe and O. M. Yaghi, J. Am. Chem. Soc., 2001, 123, 4368.
- 26 M. Safaei, H. A. Sodano and S. R. Anton, Smart Mater. Struct., 2019, 28, 113001.
- 27 H. Liu, J. Zhong, C. Lee, S.-W. Lee and L. Lin, Appl. Phys. Rev., 2018, 5, 041306.
- 28 J. Y. Fu, P. Y. Liu, J. Cheng, A. S. Bhalla and R. Guo, Appl. Phys. Lett., 2007, 90, 212907.